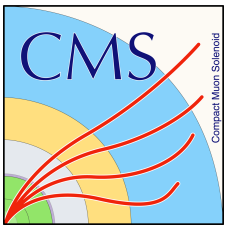

Test beam simulations of Tracker modules for the CMS Phase II Upgrade: pT triggering, efficiency, resolution.

Lorenzo de Cilladi, Università degli Studi di Torino, Italy

Supervisor: Dr. Thomas Eichhorn, CMS - DESY

18 July 2017 – 7 September 2017

Abstract

In this report, the innovative tracker modules for the CMS Phase II Upgrade are presented. Their characteristics and their operating principles are studied through the tuning both of a simulation of the test beam that will be performed at DESY, Hamburg, and of a reconstruction chain. The main feature of the new sensors – their ability to reject low transverse momentum tracks in the very early steps of the data acquisition – is tested and discussed. The alignment of the module in the test beam facility, the particle tracking and the resolution of the new sensors are studied and the results are presented.

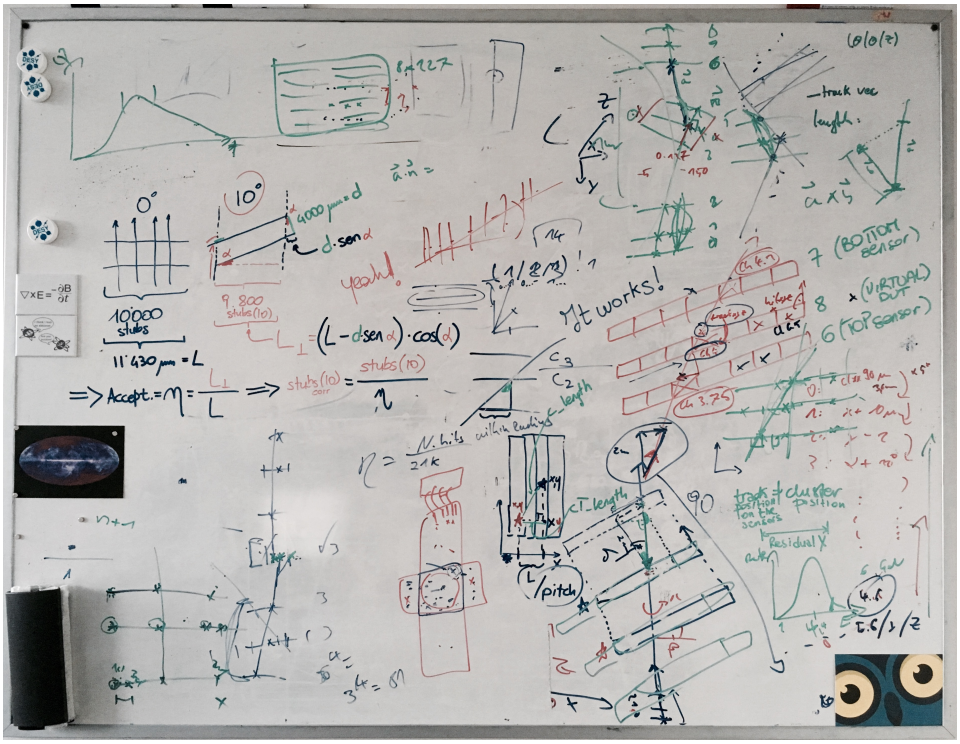

Contents

1 Introduction

The Large Hadron Collider (LHC) at CERN is going to be upgraded to the HL-LHC (High Luminosity LHC) in order to achieve an even higher luminosity. This future development will lead to an increased event rate per bunch crossing and, as a consequence, to the need for dealing with high pile-up conditions. All the experiments currently working along the LHC accelerator will need to rethink and redesign their constituent parts, with the goal of providing sufficient granularity to meet the physics performance and tracking efficiency requirements. Moreover, a higher collision rate also means an increased exposure to radiation and, therefore, to risk of damage both for the detectors and for the electronics. In this report, I will focus on the Compact Muon Solenoid (CMS) experiment. The benefits of increased luminosity will be fully exploited only if the event selection process becomes more efficient. An early rejection of low energy events is crucial for reducing the amount of data stored and processed, in order to deal with the expected event rate. The entire CMS tracking system will be renewed in the next years. The new detectors will feature several characteristics, including increased granularity (higher channel density). The innovative tracker modules for the Phase II Upgrade of the CMS experiment will be able to add tracking information to the trigger decision process, in order to ensure the rejection of low transverse momentum tracks in the very first steps of the event selection. It is crucial to implement this feature directly in the hardware because the selection algorithms become less efficient at high pile-up. The above discussed task can be carried out by the Outer Tracker of the experiment, which should be able to provide information both for the trigger decision and for the track reconstruction.
The upgraded CMS Outer Tracker will be composed of silicon detector modules called "p_T - modules", since they are capable of rejecting the tracks associated to low energy particles by exploiting the bending of their trajectories in CMS due to the magnetic field of 3.8 T. In particular, the transverse momentum threshold which is likely to be chosen is around 2 GeV/c. A more detailed description of the CMS Phase II Upgrade is given in [1].

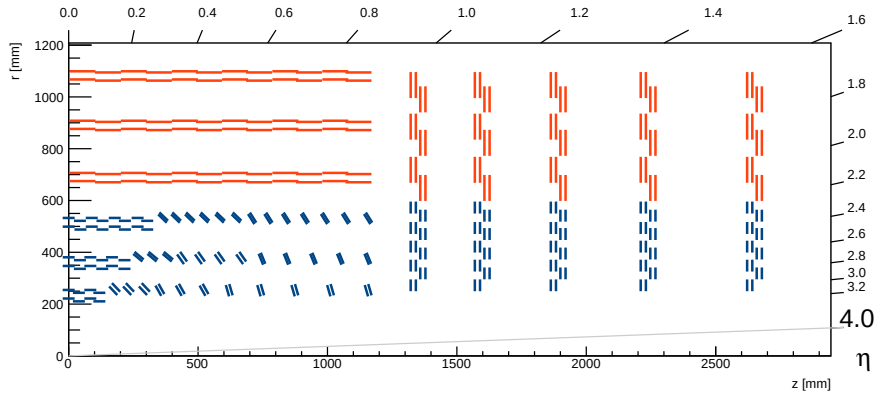

Figure 1: CMS Phase-II Outer Tracker layout design, [3]. 2S modules are shown in red, PS modules in blue.

2 The 2S module

Figure 1 shows the planned layout of the CMS Outer Tracker. PS (Pixel - Strip) modules are shown in blue, 2S (2 - Strip) modules in red. They will be placed at six different radii in the barrel region and in the outer radii of each end-cap's disks.

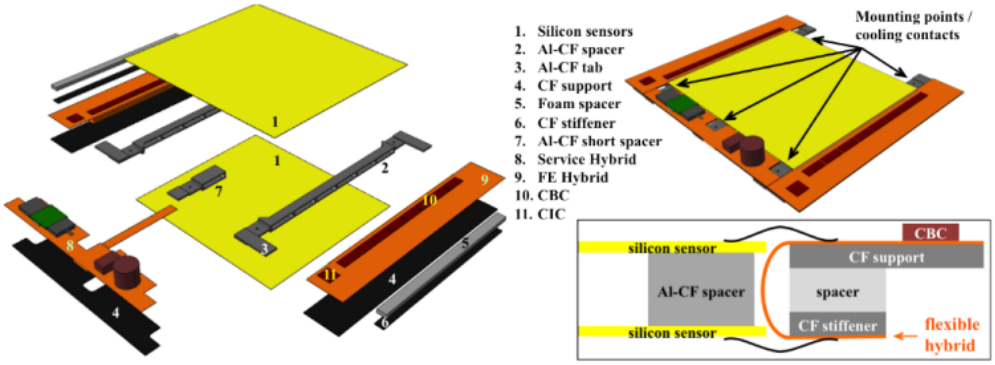

Figure 2: 2S module layout, [1].The sensor planes (in yellow), the front-end electronics – the CBC chips, at number 10 – and the support framework are shown.

The official layout of the 2S modules is shown in Figure 2. The two superimposed silicon sensors (shown in yellow) are both divided into two halves, with each side being read out by eight CBC (CMS Binary Chip), which constitute the front-end electronics. Each sensor has 8x127 silicon micro-strips. Two superimposed sensors make up a single 2S sensor: the micro-strips of each plane are perfectly aligned with those belonging to the other plane. In Table 1 and in Figure 3, geometrical specifications are given. Sensors with an inter-planar distance of 4mm (1.8mm) will be referred to as 2S 4mm sensors (2S 1.8mm sensors). The modules under test are digital sensors: any time the collected charge in a single channel exceeds a certain set threshold, the strip will give a signal of fixed height, independently of the effective value of the collected charge. If the threshold is not reached, that signal would not be produced. This behaviour is called binary operation.

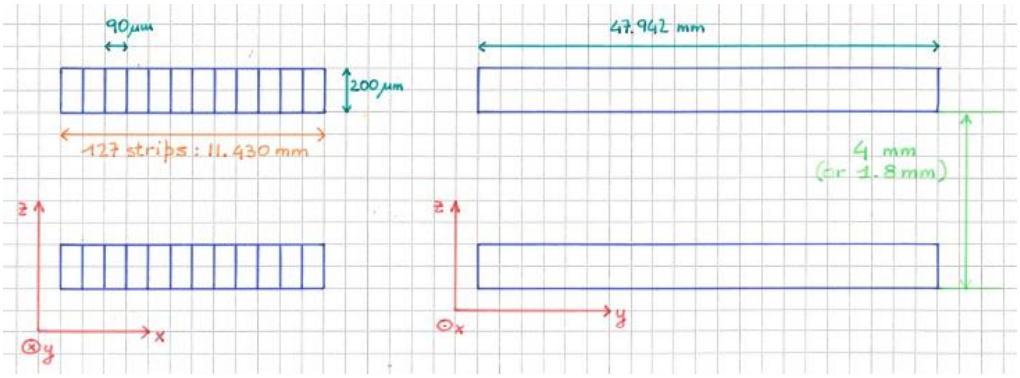

Figure 3: Geometrical specifications of that part of the sensor read out by one CBC chip. Left: section on the xz-plane. Right: section on the yz-plane.

Table 1: 2S sensor specifications

Strips per plane	8x127
Pitch	90 μm
Total thickness	320 μm
Sensitive thickness	200 μm
Strip length	47.942 mm
Inter-planar distance	4.0 mm or 1.8 mm

At DESY laboratories, a module of a 4 mm sensor has been designed and is currently being realized. As soon as the test framework will be ready, the sensor will undergo a test beam at the DESY facility in Hamburg (see Figure 4). To extract the beam from DESY II synchrotron, a fiber target is inserted in the accelerator ring along the beam line; the electron beam, hitting the target, generates a photon beam by bremsstrahlung. The photons end their track on a converter hosting another target and they are converted into e^- and e^+. An electron beam is then extracted with a dipole magnet and a collimator and reaches the Device Under Test (DUT) – the 2S module, in this case. The telescope shown in Figure 5, which includes six silicon pixel detectors, will be used for the test beam. The DUT will be placed between the three "top" and the three "bottom" telescope detectors, whose aim is to help tracking the particles of the electron beam used to test the module. The main goal of the test will be the determination of the sensor's performance in rejecting the low transverse momentum (p_T) tracks and, thus, in giving a trigger decision.

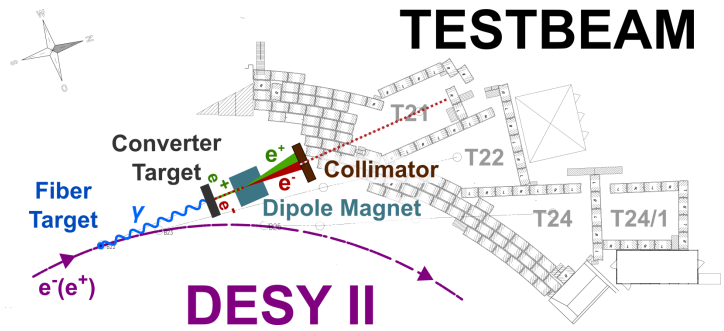

Figure 4: DESY test beam facility, [5]

Figure 5: Telescope at the DESY test beam facility

3 Simulation

Before starting the test beam and in order to study the behaviour of the 2S module, it is necessary to develop and to calibrate a simulation of both the telescope and the DUT. The simulation program *Allpix* has been used for this purpose. As it was originally

written to simulate a test beam performed on a single-layer pixel detector, some parts of the program have been modified in order to tune the simulation according to the new sensors' characteristics. In Figure 6, the simulated telescope and DUT are shown, together with a particle track. Let the telescope axis and the beam line be parallel to the z-axis of the reference frame used and the strips be along the y-axis (vertical in the above mentioned figure). Therefore, the y-coordinate is unsensitive, while the x-coordinate is the sensitive one (see Figure 3). The electrons in the simulated beam have a Gaussian distributed energy spectrum with a mean value of $E_{mean} = 5.0$ GeV and a width of $\sigma_E = 0.1$ GeV, corresponding to actual conditions at DESY Test Beam.

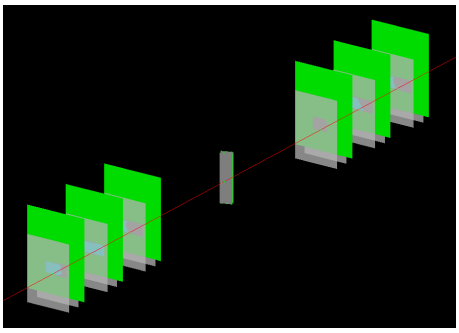

Figure 6: Simulated DUT and telescope

It is interesting to point out how the bending of the trajectories is simulated. As shown in Figure 7, the tracks of charged particles in CMS are bent due to the magnetic field generated by a superconducting solenoid. In the test beam facility, in order to be able to follow the particles' trajectories using the pixel detectors in the telescope, the geometry of the beam and of the telescope itself is linear. Therefore, instead of bending the beam, the incidence of bent trajectories on the 2S module is reproduced by inclining the 2S module inside the telescope. The two superimposed sensors are rotated around a common axis parallel to the y-axis and going through the symmetry centre of the 2S module in the xz-plane. The rotation around this axis, which will be referred to as the y-axis throughout this report, is expressed by the angle β. A rotation of the two sensors around a common axis requires to set proper shifts along the x-coordinate and the z-coordinate (see Figure 9) to maintain the alignment of the corresponding strips belonging to the two superimposed sensor planes – necessary for the low pT track rejection, as discussed in Section 4.2.

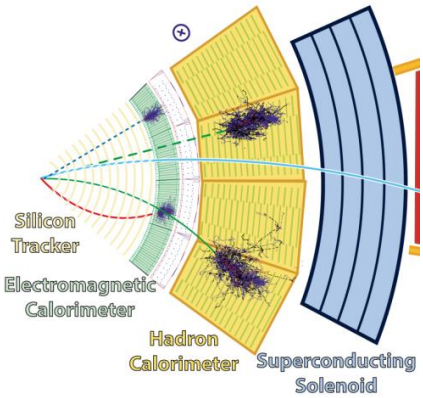

Figure 7: Track bending in CMS, [4]

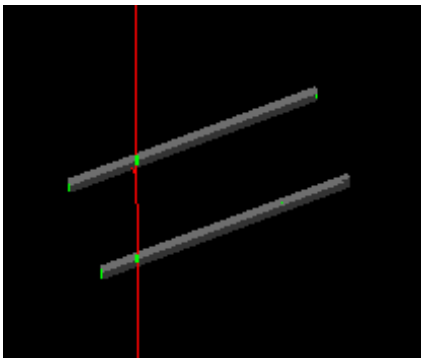

Figure 8: Track bending in the simulation

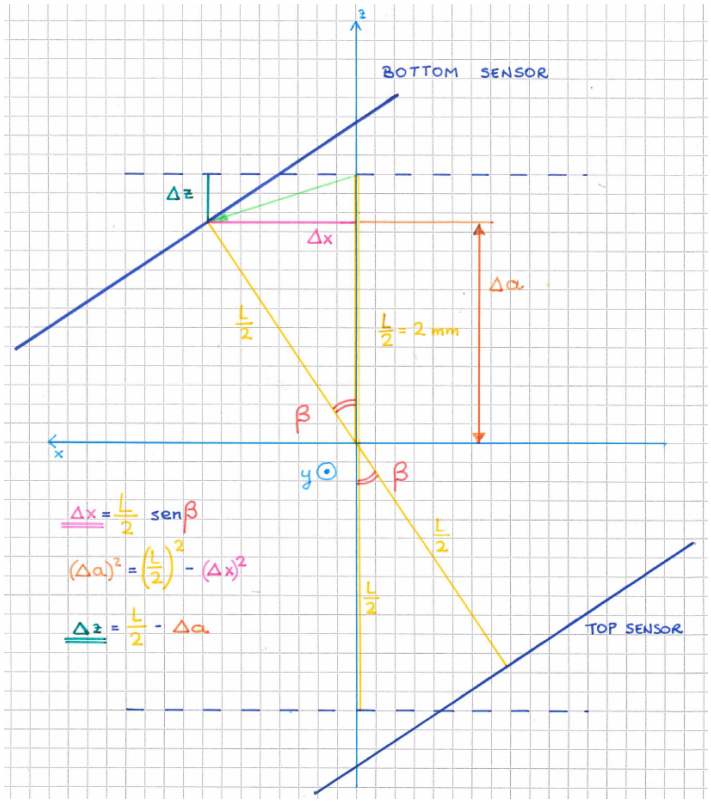

Figure 9: Rotation and shifts of the 2S module in the test beam telescope's simulations

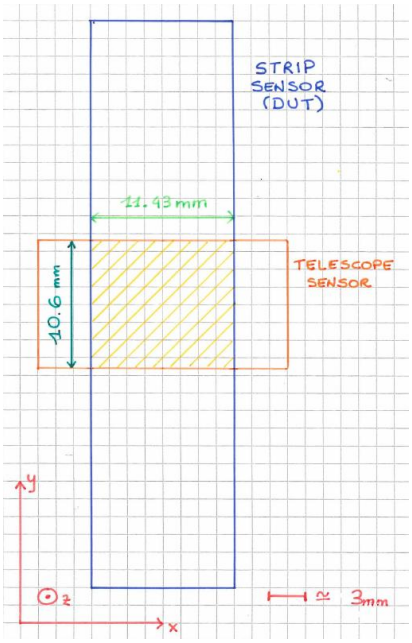

Figure 10: Strip sensor (DUT) and telescope pixel sensor: in yellow, the effective beam area

4 Reconstruction

Starting from the simulated data or from those collected during a real test beam, the reconstruction algorithm goes through many steps: in this report we will discuss the main ones, shown in the flow chart in Figure 11. The generic pixel telescope data analysis framework called "EUTelescope" is the original reconstruction program on which all the necessary changes and extensions have been performed.

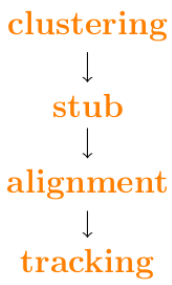

Figure 11: Reconstruction flow chart

4.1 Clustering

When a particle traverses the 2S module, if the deposited energy is enough, a cluster will be made on each of the sensor planes that were hit. A cluster is the ensemble of the contiguous channels in which the collected charge reached or exceeded a certain fixed threshold. As shown in Figure 12, the expected cluster size, given the geometry of the strips, is of 1 channel (CH) for an incidence angle $\beta = 0°$ and of 2 CH for $\beta \sim 24.2°$. The cluster size depends not only on the beam inclination with respect to the sensor plane, but also on the charge sharing between the contiguous channels. A spherical propagation of the charge around the impact point, decreasing with the square power of the distance, seems to be a reasonable approximation. Therefore, the charge sharing in the simulations has been made quadratically position dependent: the percentage of charge shared (scp) with a neighbouring strip is equal to zero if the hit point corresponds to the middle point of the strip itself (along the sensitive coordinate X) and to a certain maximum amount (scp_{max}) if the hit is on the border between two sensors. The function that describes the variation of the shared charge percentage is a quadratic function of the position: $scp = \frac{scp_{max}}{(p/2)^2}\, x^2$, where p is the strip pitch ($p = 90\mu$m).

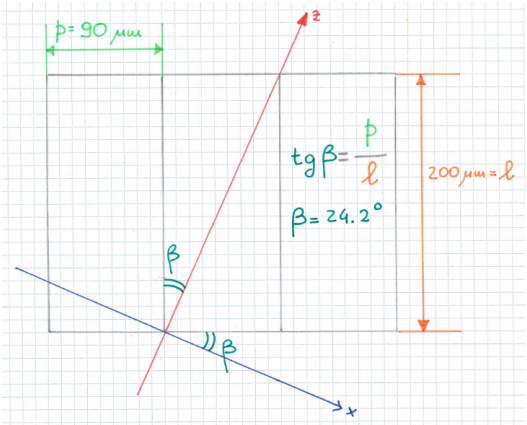

Figure 12: Charge sharing tuning angle

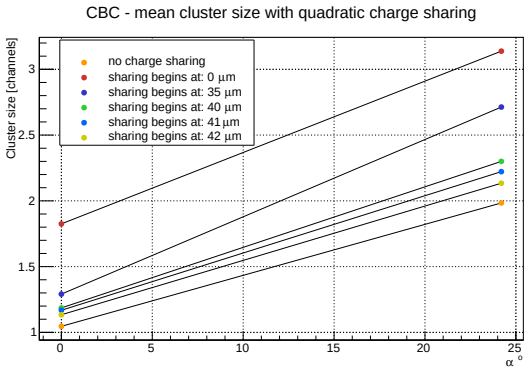

Figure 13: Cluster size optimisation

In Figure 13, different attempts for obtaining the desired cluster size are shown: scp_{max} is set to 0.4, and the different points represent a charge sharing area starting at different distances from the strip edges. In order to reach the expected cluster size, it appears to be better to let the charge sharing happen only in the region next to the edges of each strip. The comparison with measurements taken in the test beam will give more information about the actual cluster size and will enable the charge sharing to be tuned more accurately.

4.2 Stub

In this section, one of the main feature of the 2S modules, the rejection of low transverse momentum tracks, is explained. At this point of the reconstruction flow, information

about the hit cluster size and position on each strip sensor in channel (CH) coordinates and in global coordinates are known. We also know where the particles hit the telescope sensors in each recorded event.
Now follows the stub process, which allows low p_T tracks to be rejected. As already discussed, both in the simulation and in the real test beam the bending of the particle trajectory is emulated by rotating the 2S sensors (see Figure 9). Since the CMS magnetic field of $B = 3.8$ T has a different bending effect on particles with different transverse momentum, it is possible to define a $\beta \leftrightarrow p_T$ conversion at three different modules' radii (cf. the red layers in Figure 1). Let R_1 (687.000 mm) be the radius of the innermost position of 2S modules in the outer tracker, R_2 (888.792 mm) the radius of the middle position and R_3 (1080.000 mm) the radius of the outermost position. At a fixed radius R and with a bending magnetic field B, the conversion between the inclination β and the transverse momentum p_T is

$$p_T[GeV/c] \;=\; 0.3 \cdot B[T] \cdot \frac{R\,[m]}{2 \sin \beta}$$

Different p_T means different bending: if a particle has a higher transverse momentum, then the trajectory will be straighter; if the p_T is lower, the track will be more bent, and this will let the read-out electronics reject the track.

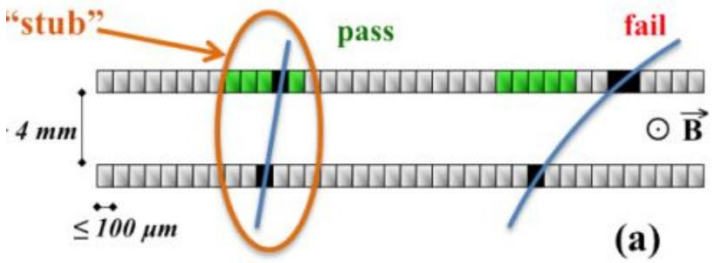

Figure 14: Stub process, [1]

The stub process is shown in Figure 14. A track is accepted – a stub is made – if the following relation is satisfied:

$$\text{if } (|hit_{Top} - hit_{Bottom}| < \text{stub window}) \text{ [in CH coordinates]} \Rightarrow \text{make a } \textbf{stub},$$

where (see also Figure 15):

- hit_{Top} is the hit position on the top sensor in channel coordinates,
- hit_{Bottom} is the hit position on the bottom sensor in channel coordinates,
- stub window is half of the total acceptance window (green in Figure 14); the stub window size is directly set in the module's electronics, in integer CH coordinates,
- stub is a "flag": if a track is accepted, then a stub is made; if a track is rejected, the stub is not made.

The stub process is the main innovative feature of the 2S modules; if a stub is made, then the 2S module, in the future CMS Outer Tracker, will send a trigger decision, letting only the events with a sufficient p_T be stored for further analysis. Indeed, setting a stub window will automatically reject the tracks with a p_T below a certain threshold, as their trajectory will be more bent by the magnetic field and the hit on the bottom sensor will fall out of the acceptance window. In order to make the selection process work properly, the strips of the two superimposed sensors need to be aligned with a very high precision. Possible misalignments can be corrected using an offset in order to shift the stub window on the bottom sensor; this feature has been implemented in the reconstruction code.
Since the $\beta \leftrightarrow p_T$ conversion depends on the radius R of the tracker's layer, a fixed stub window means a different track inclination acceptance at the different radii and, therefore, a different p_T threshold. Conversely, at a fixed radius, it is possible to vary the p_T threshold by changing the width of the stub window: a larger window will allow also lower p_T tracks to be accepted. A transverse momentum threshold of $\sim$2GeV/c is likely to be chosen at CMS after the installation of the HL-LHC.

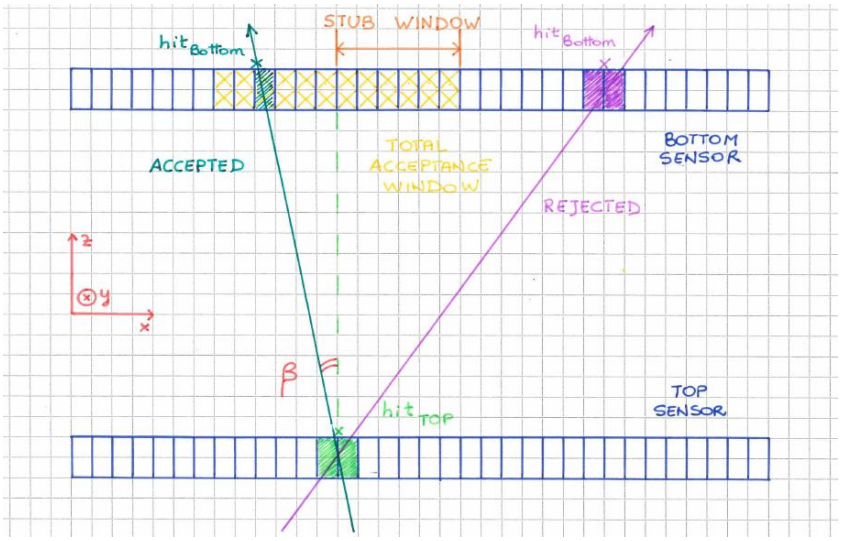

Figure 15: Stub window

In order to test if and how this track selection works, test beam simulations have been performed at various DUT inclinations β, corresponding to different p_T at the different radii. Then, the stub counter has been implemented in the reconstruction program; the number of tracks accepted has been counted for each simulated data set, varying the stub window width. The values obtained for different β and with different stub windows are shown in the table in Appendix (section 7); there, the stub window that sets the threshold at around 2 GeV/c for modules at the innermost radius is highlighted in red. The same is done for the medium radius (green) and the outermost radius (blue).

The plots in Figures 22(a), 22(b) and 22(c) show the stub efficiency (or track acceptance efficiency) as a function of the transverse momentum. The efficiency is defined as the number of stubs counted (or of accepted tracks) divided by the number of stubs made

at 5° – except for the case of stub window sizes equal to 1, 2, 3, 4 CH, for which the number of tracks accepted at 0° was used for the normalization; this is because if these window sizes are set, the cutoff, at an inclination of 5°, has already happened. The plots confirm that the stub process for rejecting low transverse momentum events works: the track acceptance efficiency rapidly falls to zero at a certain p_T value, representing the threshold. The plots are a clear indication on how changing the stub window, at a fixed radius, has as a result the shift of the p_T cut: the larger the window, the lower the threshold. It is worth noticing that the shifts in the threshold caused by unitary change of window width are discrete, because the stub window width is an integer value. Moreover, the plotted points are not continuous and, if connected, they appear as broken lines; this is because the simulated data sets that have been used refer to a limited number of inclinations β. If more of them had been used, with smaller $\Delta\beta$ between each other, the plots would appear smoother; nevertheless, this is actually not really important, as the mechanical precision in positioning the 2S module at different inclination in the test beam telescope will be 0.5° at best.
In each of the three plots in Figure 22(d), 22(e) and 22(f), the stub window width is fixed and the cutoff positions at the different radii are shown. In order to get a cutoff at $p_T = 2\,\mathrm{GeV/c}$ for a 2S 4mm sensor, the required stub window widths are

- 9 CH at $R_1 = 687.000\,\mathrm{mm}$,
- 12 CH at $R_2 = 888.792\,\mathrm{mm}$,
- 14 CH at $R_3 = 1080.000\,\mathrm{mm}$.

When increasing the radius, moving towards the outer region, the threshold for a certain fixed window shifts to higher p_T.

Normalization and corrections

Since only the particles – the tracks – which hit both the sensor planes undergo the stub process and can contribute, if accepted, to the next steps of the reconstruction chain, a geometrical acceptance of the DUT needs to be defined and to be used in order to normalize the number of stubs made, or of tracks accepted.
When the beam is perpendicular to the DUT planes, all the tracks that hit the top sensor will go through the bottom sensor too – with some exceptions due to scattering or beam divergence – and will therefore participate in the stub process. As shown in Figure 16, when the module's planes are not orthogonal to the beam, a fraction of the tracks will intersect only one of the two DUT planes; the corresponding hits won't contribute to the stub process and to the following steps of the reconstruction flow. This reflects in a decrease of the number of tracks accepted, which becomes smaller as the inclination β increases, even if the transverse momentum is higher than the p_T threshold. In order to eliminate this effect, a geometrical acceptance has been defined as $\eta = \frac{L_\perp}{L}$, where

- $L_\perp$ is the length along the x-direction of the 2S module's transverse section shared by both of the two superimposed sensors (see Figure 16);

- L is the total length of each sensor along the sensitive coordinate in the configuration where $\beta = 0°$, or the transverse section shared by the two sensors at $\beta = 0°$.

The number of accepted tracks normalized by geometrical acceptance is equal to the non-normalized number of stubs (shown in the table in Appendix, section 7) divided by the acceptance η at the respective inclination β.

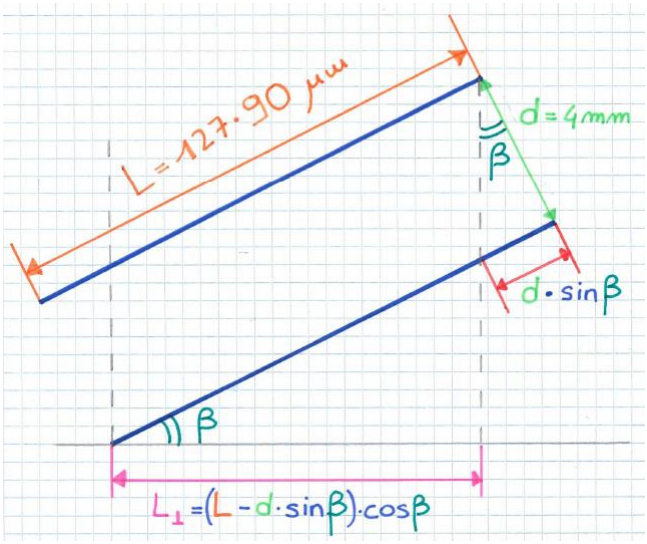

Figure 16: Geometrical acceptance

By looking at the data shown in the above mentioned table in the regions far from the cutoffs, it is possible to notice that there is an increase in the number of tracks accepted of circa 4 (on average) per each channel the stub window is made larger (if the stub window is increased by 1 CH, then the total track acceptance window is enlarged by 2 CH, one per each side with respect to the hit position). This effect is most likely caused by the beam divergence and by the scattering of the beam particles that can occur in in the telescope or in the sensors themselves. This number of additional accepted tracks can be subtracted from the total number of tracks shown in the table in Appendix.

The six plots shown in Figure 23 in the Appendix (section 7) are the same plots presented in Figure 22 and described above, but with both the geometrical acceptance normalization and the beam divergence and scattering correction applied. Thanks to these corrections, the stub efficiency becomes higher and constant (at the value of ~ 1) in the regions above the p_T thresholds, since the geometrical effect reducing the efficiency of the sensor has been compensated for. The plots in Figure 23(d), 23(e) and 23(f) allow an important observation: a fixed window size will set different thresholds at different radii. Nonetheless, a constant threshold throughout the detector is desired. Therefore, we have to set the stub window for each single module according to its position in the CMS Outer Tracker in order to tune the p_T cutoff; we can obtain, thus, a p_T threshold as homogeneous as possible throughout the whole tracker.

4.3 Alignment, tracking, resolution

The last steps performed in the reconstruction chain are the alignment of the module under test and the tracking of the particles going through the telescope. The track reconstruction is conducted using the information about the recorded hits on the telescope pixel sensors. This process is exemplified in Figure 17 and is explained here.

1. Let us focus on one of the two telescope triplets: a track is extrapolated from the hits on the first and the third telescope sensors belonging to that triplet.

2. If the intersection between the extrapolated track and the second telescope plane is close enough to the actual recorded hit on this plane (within a certain acceptance window, shown in pink in Figure 17), then this "triplet track" is accepted.

3. The same procedure explained at the points 1. and 2. is repeated for the other telescope triplet.

4. An attempt to match the two tracks in a certain region between the two triplets is carried out; if this happens, within a certain acceptance window (green in Figure 17), then the matched track is accepted, if it fulfills a certain $\frac{\chi^2}{\mathrm{NDF}}$ criteria.

If a matched track is accepted, the alignment step will be performed. A simplified alignment procedure has been adopted (see Figure 18).

1. Instead of aligning the two DUT sensors separately, and since the position of the two sensors with respect to each other is known very well by construction (the mechanical precision of their positioning should allow making this assumption), a virtual sensor plane is generated exactly in the middle of the two real sensors, at a distance of 2 mm from each one of them.

2. Starting from the clusters and the corresponding hits on the two real sensors (that we already know at this point of the reconstruction chain), a **virtual** cluster and **hit** (pink in Figure 18) are created on the virtual plane.

3. The virtual plane is aligned using the reconstructed track and the virtual hit as a reference; shifts in the x-coordinate and y-coordinate and rotations around the z-axis are allowed.

4. After the alignment is completed, the intersection between the reconstructed track and the virtual sensor is calculated and called **virtual track hit**.

5. As the position of the real planes with respect to the aligned virtual sensor is well-known, the track hits' positions on the real planes are calculated back from the virtual track hit's position.

Let the **residual in x** be the distance along the x-coordinate between the virtual hit and the virtual track hit. If the residual in x is computed for a certain amount of events at a fixed inclination, its distribution will be like the one shown in Figure 19,

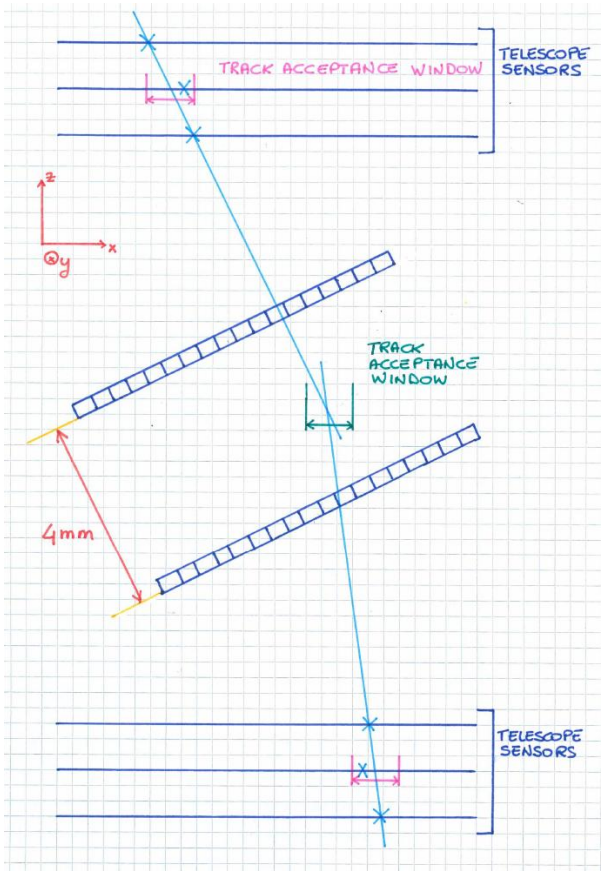

Figure 17: Track reconstruction

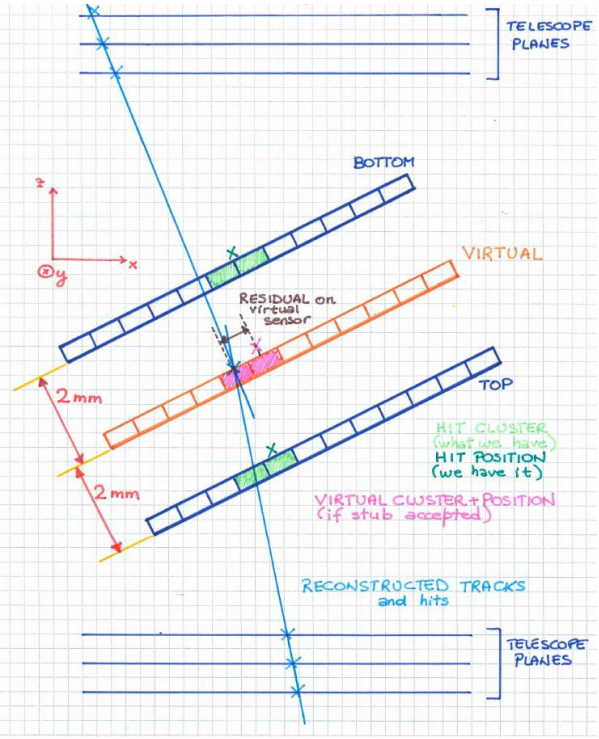

Figure 18: Alignment and residual

where $\beta = 20°$. The histogram is fitted with a Gaussian function. The sigma σ of the distribution represents the resolution of the 2S module's sensors; its trend at different incidence angles β is shown in Figure 20. At $\beta = 0°$, the resolution is $\sigma = 29.0\,\mu$m; at $\beta = 20°$, the resolution is $\sigma = 16.8\,\mu$m.

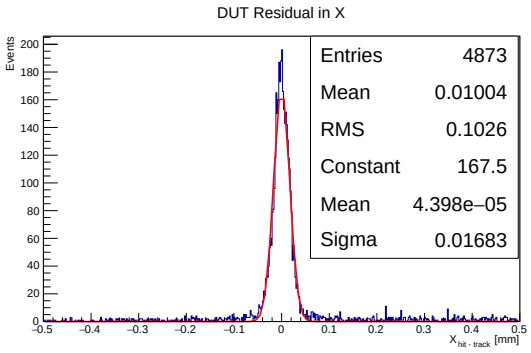

Figure 19: Distribution of the residual in x

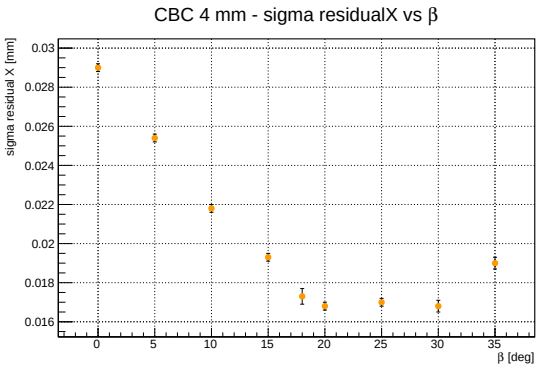

Figure 20: Residual in x vs inclination β

5 Efficiency

The last part of this report concerns the definition of the 2S module's tracking **efficiency**, the first studies on it and the outlook for further future developments of its analysis. Let a **valid track hit** be the intersection between an accepted reconstructed track in the test beam telescope (see Section 4.3). and the virtual sensor; this definition excludes all those tracks that, although accepted, do not intersect the DUT. Let also a **matched DUT hit** be a virtual hit (defined in Section 4.3) that has been matched, within a certain matching acceptance window, to a valid track hit – notice that a virtual hit is created only if two hits on the real sensors were recorded and were accepted during the stub process. Each virtual hit can be matched with only one valid track hit – and vice versa –, in particular the closest one. The matching acceptance window is the combination of two one-dimensional acceptance windows: the maxDistY and the maxDistX. They are, respectively, the maximum distances along the y-coordinate and along the x-coordinate between a valid track hit and a virtual hit that allow a virtual hit to be accepted as a matched DUT hit. The maxDistY extends along the unsensitive coordinate, so it has been fixed at the reasonably large value of 10 mm – large with respect to the 90 μm pitch of the strips. The tracking efficiency ε of the 2S module is defined as

$$\varepsilon = \frac{\#\,\text{matched DUT hits}}{\#\,\text{valid track hits}}$$

The plot in Figure 21 shows the dependence of the tracking efficiency on the maxDistX. The orange points have been obtained using a simulation with $\beta = 5°$ in which only one particle per each event traverses the telescope. The green points refer to a simulation, again at $\beta = 5°$, in which the number of particles per event follows a Gaussian distribution with the mean value equal to 3 and the width equal to 1. The efficiency is almost constant if the maxDistX is about as large as the pitch or greater. In order to avoid wrong matching, the maxDistX should be set at the minimum value that allows the efficiency be equal to the constant maximum value.

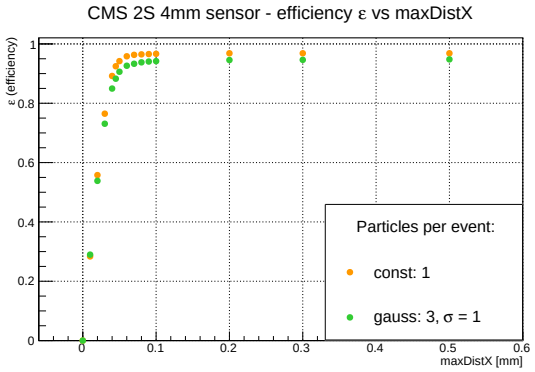

Figure 21: 2S sensor tracking efficiency

One more observation can be made. The resolution of our sensors at a certain inclination β is equal to the width σ of the distribution of the residual in x, as discussed in Section 4.3.

At $\beta = 5°$, the resolution is approximately $25.4\,\mu$m (see Figure 20). The maxDistX window works on the same quantity that has been defined as residual in x. Therefore, setting a maxDistX equal to 1σ, will let only $\sim 68.3\,\%$ of the DUT hits be matched with the respective valid track hits. Following this reasoning, a maxDistX of 2σ (circa $50.8\,\mu$m at $\beta = 5°$) or of 3σ (approximately $76.2\,\mu$m at the same inclination) corresponds respectively to $\sim 95.5\,\%$ and to $\sim 99.7\,\%$ of accepted matched hits. This percentages, which are properties of the normal distribution ([6]), are obtained as efficiencies if the maximum value of efficiency reached is redefined as $100\,\%$. It is possible to conclude that, reducing the maxDistX beyond three times the resolution introduces a resolution effect that causes the fall in the tracking efficiency.

The two sets of points do not reach the same maximum efficiency. This is due to the fact that when the number of beam particles per event is greater than one, more than one hit per event is recorded on each telescope sensor. Therefore, the number of possible combination of the hits on the telescope sensors that can be used to reconstruct the tracks rapidly increases, together with the risk of accepting wrong tracks. In order to increase the efficiency, in particular when the multiplicity is greater than one, additional constraints on the track reconstruction process can be studied and implemented. By doing so, it might be possible to avoid using wrongly reconstructed tracks and to reduce the uncertainties.

6 Conclusions and outlook

In order to reproduce the characteristics of the innovative CMS 2S tracker modules and to test their features, the existing implementations of a simulation program for the reproduction of a test beam at the DESY facility and the reconstruction chain have been modified in various parts and properly tuned. As discussed in this report, the 2S module has a good potential for rejecting tracks below a certain transverse momentum threshold and, therefore, for sending a clear trigger information. This will let the event selection be more efficient at CMS when the LHC will be upgraded to the High Luminosity LHC.

By tuning the track acceptance window – the stub window – for each module according to its position in the CMS Outer Tracker, it will be possible to set a homogeneous threshold at $p_T \sim 2\text{GeV/c}$ throughout the CMS Outer Tracker.

Further studies on the 2S module's efficiency can be conducted and more precise acceptance constraints on the track reconstruction process can be set consequently. This will avoid using wrong tracks in the alignment process and will possibly let the resolution and the efficiency improve.

Information about the telescope and the sensors' noise from previous test beam campaigns ought to be taken into account, in order to make the simulation more accurate and realistic and to fine-tune accordingly the constraints employed in the reconstruction chain.

As soon as the test beam will be performed at the DESY facility in Hamburg, all the results obtained analysing the simulated data will be compared with those coming from actual measurements. This will allow the simulation program and the reconstruction algorithm to be tuned more accurately and will help in the interpretation and analysis of measurement results.

7 Appendix

Stub counts table

In this table, the number of stubs made using simulated data is recorded. The simulations have been performed at different incidence angles β of the beam on the sensors' planes. The stub process has been conducted setting the stub window to different values (in channel units).

Stub window					Number of stubs															
			1	2	3	4	5	6	7	8	9	10	11	12	13	14	15	16	17
β [°]	$p_T(R_1)$ [GeV/c]	$p_T(R_2)$ [GeV/c]	$p_T(R_3)$ [GeV/c]																
5				10	27	64	3596	11838	11859	11870	11881	11894	11905	11918	11928	11932	11943	11950	11956	11966
6				11	24	44	104	6789	11756	11772	11783	11799	11809	11824	11833	11839	11847	11859	11864	11873
7				9	21	39	65	175	9540	11699	11728	11739	11749	11760	11775	11780	11783	11794	11801	11806
8				7	22	33	51	84	248	11571	11650	11669	11680	11690	11698	11706	11715	11724	11730	11736
9				11	24	32	42	54	86	1374	11405	11441	11454	11470	11477	11482	11488	11494	11500	11510
10	2.26			8	17	31	41	51	70	114	6398	11391	11410	11424	11431	11438	11445	11455	11459	11465
11	2.05			4	11	19	21	29	38	53	123	8733	11242	11253	11265	11273	11281	11290	11299	11304
11.5	1.96			11	22	33	43	52	57	65	101	1672	11192	11232	11250	11256	11259	11263	11268	11277
12	1.88			5	14	21	29	37	45	56	81	187	11003	11198	11210	11219	11226	11236	11245	11256
13				13	22	27	36	48	55	65	82	101	320	10964	11021	11042	11060	11063	11068	11078
14		2.09		7	16	29	39	55	59	67	84	98	125	1145	10951	10977	10994	11004	11010	11022
14.5		2.02		7	11	22	28	39	53	66	74	84	93	186	10773	10881	10901	10908	10919	10927
15		1.96		11	21	32	38	46	59	69	81	99	111	151	6660	10852	10875	10883	10893	10901
16		1.84		6	13	18	28	35	45	51	59	68	82	96	143	9209	10667	10681	10692	10705
17			2.11	9	16	29	37	42	48	56	68	74	84	92	112	193	10451	10569	10586	10593
17.5			2.05	6	14	21	28	37	50	56	65	72	76	84	93	116	3576	10548	10583	10602
18			1.99	14	25	36	40	45	56	65	70	84	89	100	117	136	280	10458	10530	10548
19			1.89	6	15	25	33	40	49	62	68	77	84	88	100	112	131	396	10305	10365
20				6	14	20	25	33	44	51	64	73	81	84	91	98	104	127	813	10163
25				8	15	25	33	39	46	49	59	64	71	78	81	96	103	108	112	120
30				8	17	22	27	36	39	46	54	58	62	65	73	83	92	102	110	117

Plots without corrections

The following plots show the dependence of the stub efficiency on the p_T of the tracks in the 2S modules without using a normalisation or other corrections.

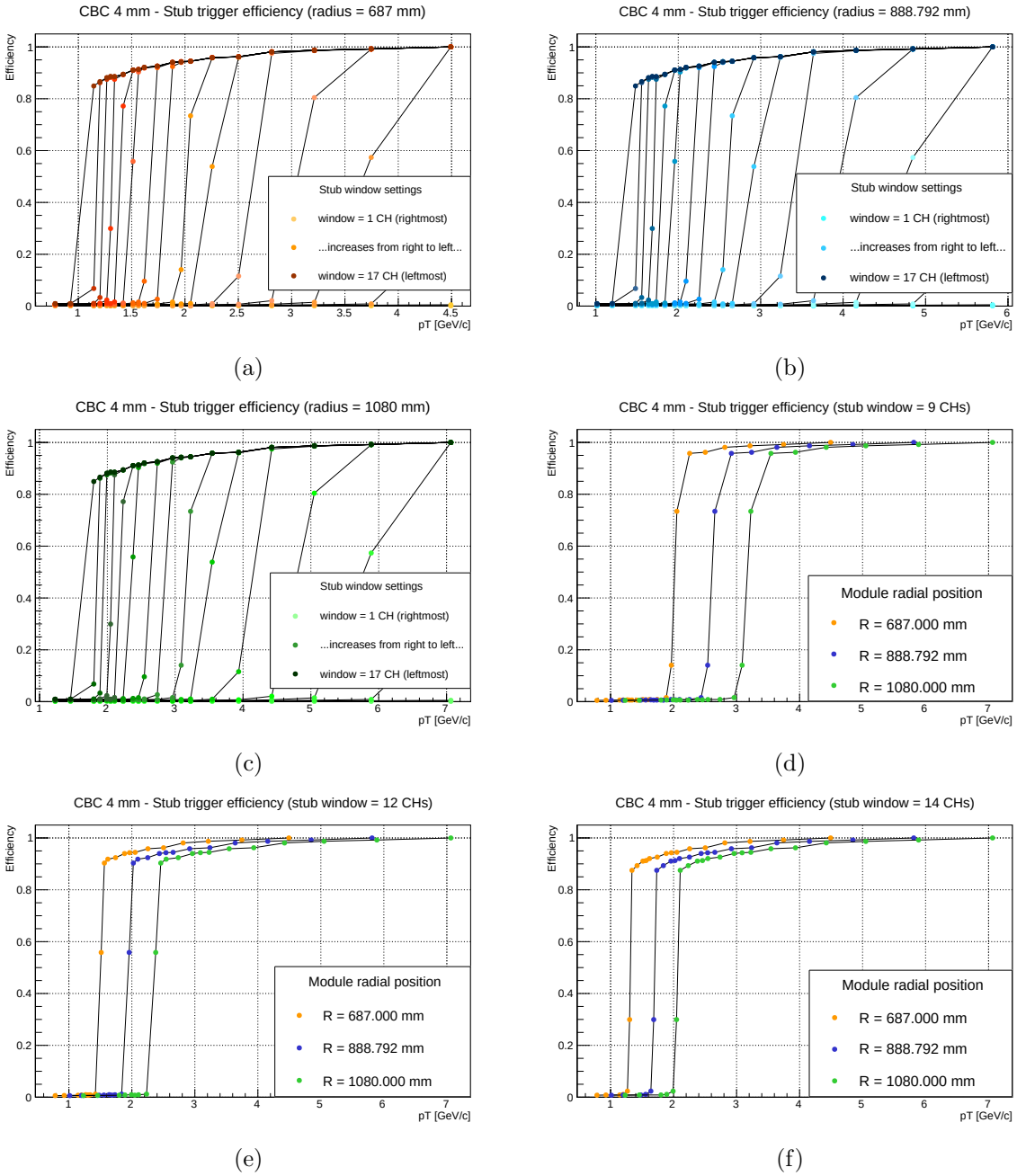

Figure 22

Plots with corrections

The following plots show the dependence of the stub efficiency on the p_T of the tracks in the 2S modules; the geometrical acceptance normalisation and the beam divergence and scattering correction have been applied.

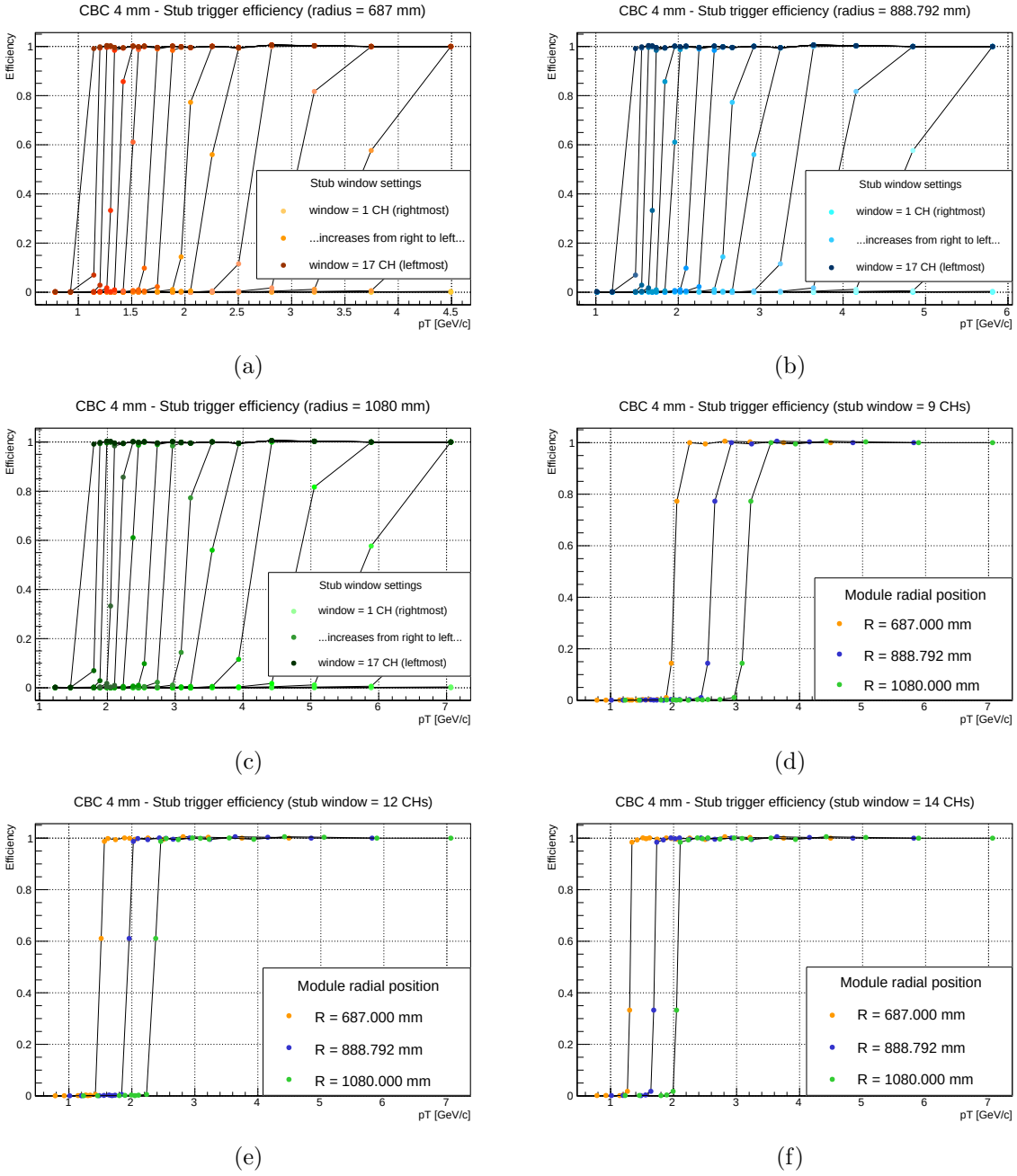

Figure 23

8 Acknowledgements

To Thomas, my supervisor, who followed me step by step in this project, always ready to give me advice and to discuss my ideas, allowing me to learn how to deal with unexpected problems and letting me make progresses in my knowledge. He trusted me and my work, for which I am grateful.

To Paul, Ali, Nikita for the advices they gave me when discussing about my project. To Doris and Andreas, for their precious suggestions at the CMS meeting.

To Olaf and to all the organising staff, for their perfect job.

To Professors Ada Solano and Marco Costa, for allowing me to know about this Summer Program and for following me in the application procedures. And to the professors and researchers, in particular to Gianna Vivaldo, who enthusiastically supported my decision to apply for this program.

To Marco, Ceren, Meadhbh, Felix. Their friendship is special to me. We shared every moment of our lives at DESY. Together we worked and we relaxed, we travelled and we discovered, we cooked and we enjoyed. We shared happiness and tiredness. But we always were there for each other. Danke schön!

To all the Summer Students who shared with me this program at DESY. You have been like a family.

To my family and my friends from Italy. Someone travelled hundreds of kilometres to come and visit me; someone called me or sent me messages to hear from me and to keep in contact. My mother, brother and grandmother supported me in a moment of uncertainty, and so did my friends, fortunately. They allowed me to participate in an experience incredibly important to me.

References

[1] *CMS collaboration*, Technical proposal for the Phase-II Upgrade of the Compact Muon Solenoid, CERN-LHCC-2015-10 / LHCC-P-008, CMS-TDR-15-02

[2] A. *Harb et al. on behalf of the CMS collaboration*, Test beam results of the first CMS double-sided strip module prototypes using the CBC2 read-out chip, *Nuclear Instruments and Methods in Physics Research A*, 845 (2017) 93–96

[3] `http://mersi.web.cern.ch/mersi/layouts/current/`

[4] *S. R. Davis (The CMS Collaboration)*, Interactive Slice of the CMS detector, `https://cds.cern.ch/record/2205172?ln=en`, *CMS-Outreach-2016-027*

[5] `http://particle-physics.desy.de/e252106/e252106/e252211`

[6] *G. Cannelli*, Metodologie sperimentali in Fisica, *Edises*, 2010